Supplementary material for

Optimal Deep Brain Stimulation Sites and Networks for Cervical vs. Generalized Dystonia

Authors

Andreas Horn*[1-3], Martin Reich*[4], Siobhan Ewert*[1], Ningfei Li[1], Bassam Al-Fatly[1], Florian Lange[4], Jonas Roothans[4], Simon Oxenford[1], Isabel Horn[1], Steffen Paschen[5], Joachim Runge[6], Fritz Wodarg[7], Karsten Witt[8], Robert C. Nickl[9], Matthias Wittstock[10], Gerd-Helge Schneider[11], Philipp Mahlknecht[12], Werner Poewe[12], Wilhelm Eisner[13], Ann-Kristin Helmers[14], Cordula Matthies[9], Joachim K. Krauss[6], Günther Deuschl[5], Jens Volkmann[4], Andrea A. Kühn[1]

Author Affiliations

1. Movement Disorder and Neuromodulation Unit, Department of Neurology, Charité – Universitätsmedizin Berlin, corporate member of Freie Universität Berlin and Humboldt- Universität zu Berlin, Department of Neurology, 10117 Berlin, Germany
2. Center for Brain Circuit Therapeutics Department of Neurology Brigham & Women's Hospital, Harvard Medical School, Boston MA 02115, USA
3. MGH Neurosurgery & Center for Neurotechnology and Neurorecovery (CNTR) at MGH Neurology Massachusetts General Hospital, Harvard Medical School, Boston, MA 02114, USA
4. Julius-Maximilians-University Würzburg, Department of Neurology, Germany
5. University Kiel, Department of Neurology, Germany
6. Department of Neurosurgery, Medical School Hannover, MHH, Hannover, Germany.
7. University Kiel, Department of Radiology, Germany
8. University Oldenburg, Department of Neurology, Germany
9. Julius-Maximilians-University Würzburg, Department of Neurosurgery, Germany
10. University Rostock, Department of Neurology, Germany
11. Charité – Universitätsmedizin Berlin, corporate member of Freie Universität Berlin, Humboldt-Universität zu Berlin, and Berlin Institute of Health, Department of Neurosurgery, Berlin, Germany.
12. Department of Neurology, Innsbruck Medical University, Austria
13. Department of Neurosurgery, Innsbruck Medical University, Austria
14. University Kiel, Department of Neurosurgery, Germany

Corresponding Author

Andreas Horn, MD, PhD
Movement Disorders & Neuromodulation Unit
Department of Neurology
Charité – Universätsmedizin Berlin
Charitéplatz 1
10117 Berlin
andreas.horn@charite.de

Further anatomical considerations

The following considerations went into forming the hypothesis of the present manuscript, that have only briefly been touched upon in the introduction and **figure 1** (main text):

Together with the reticular part of the substantia nigra (SNr), the GPi constitutes the *output ganglion* of the basal ganglia, feeding *cortical* signals that arrived at the striatum and external pallidum (GPe) via the thalamus back to the cortex (1–3). This loop model has become fundamental in our understanding of movement disorders such as dystonia, Parkinson's Disease and other *'basal ganglia disorders'*. Multiple refinements of this model have been proposed since (4–6) and converging models have been developed in parallel within the basal ganglia and reinforcement learning fields (see **Fehler! Verweisquelle konnte nicht gefunden werden.** A for an example). These models have often been defined in form of boxes and arrows to show *functional* interactions between structures. Concepts such as the direct, indirect and hyperdirect pathways (7, 8) have become fundamental for our understanding (5), but are primarily functional concepts. While their anatomical correlates have been investigated (7, 9–12), in the larger body of functional basal ganglia studies, less focus has been put on the exact tracts that implement direct and indirect pathways (including their projections back to thalamus and cortex).

To derive at a circuit-based hypothesis of DBS in anatomical space, a translation to specific anatomical structures is necessary (**Fehler! Verweisquelle konnte nicht gefunden werden.** B). One component that has been well characterized on an anatomical level is the hyperdirect pathway. Parts of descending glutamatergic projections from cortex to the motor pattern initiator / generator networks in the brainstem (4) send axon-collaterals to multiple subcortical regions such as the subthalamic nucleus (STN) which functionally define what we call the hyperdirect pathway (7, 8, 12). Anatomical correlates of the direct and indirect pathways are intermixed and implemented via i) the striatopallidofugal bundle and ii) Edinger's comb system. The former, a massive white-matter structure that traverses the striatum (in form of Wilson's pencils (13, 14)) and both parts of the pallidum radially while partly rewiring in the laminae externae, internae and accessoriae (**Figure S1 B**), hence partly forming indirect pathway (synapsing within GPe) and direct pathway (projecting from striatum directly to GPi). Another crucial functional component of the indirect pathway is the STN which is connected via an extension of the striatopallidofugal system that traverses the internal capsule orthogonally and forms part of the comb system of Edinger (14, 15). Macroscopically, the same structure also shows connections between striatopallidal regions

and the SNr. Finally, pallidothalamic fibers are traversing the pallidum in *orthogonal* fashion to the striatopallidofugal system. One reason could be that terminal fields of pallidal neurons that integrate information from striatal domains are arranged in a disc-like fashion orthogonal to the striatopallidofugal bundle (**Figure S1**). Crucially, these disc-like receptive fields of pallidal neurons are of *fixed size* and hence integrate information from increasingly larger striatal (and hence cortical) zones medially (4, 9, 10). Hence, increasingly medial pallidal neurons (even within the GPi) seem to form the largest integrator hub regions within the pallidum. Finally, a quite exclusive property of the STN is that it has no known direct efferents to the thalamus, i.e., its feedback to the loop is indeed quite indirect (while the GPe does project to the thalamus, directly; (4)).

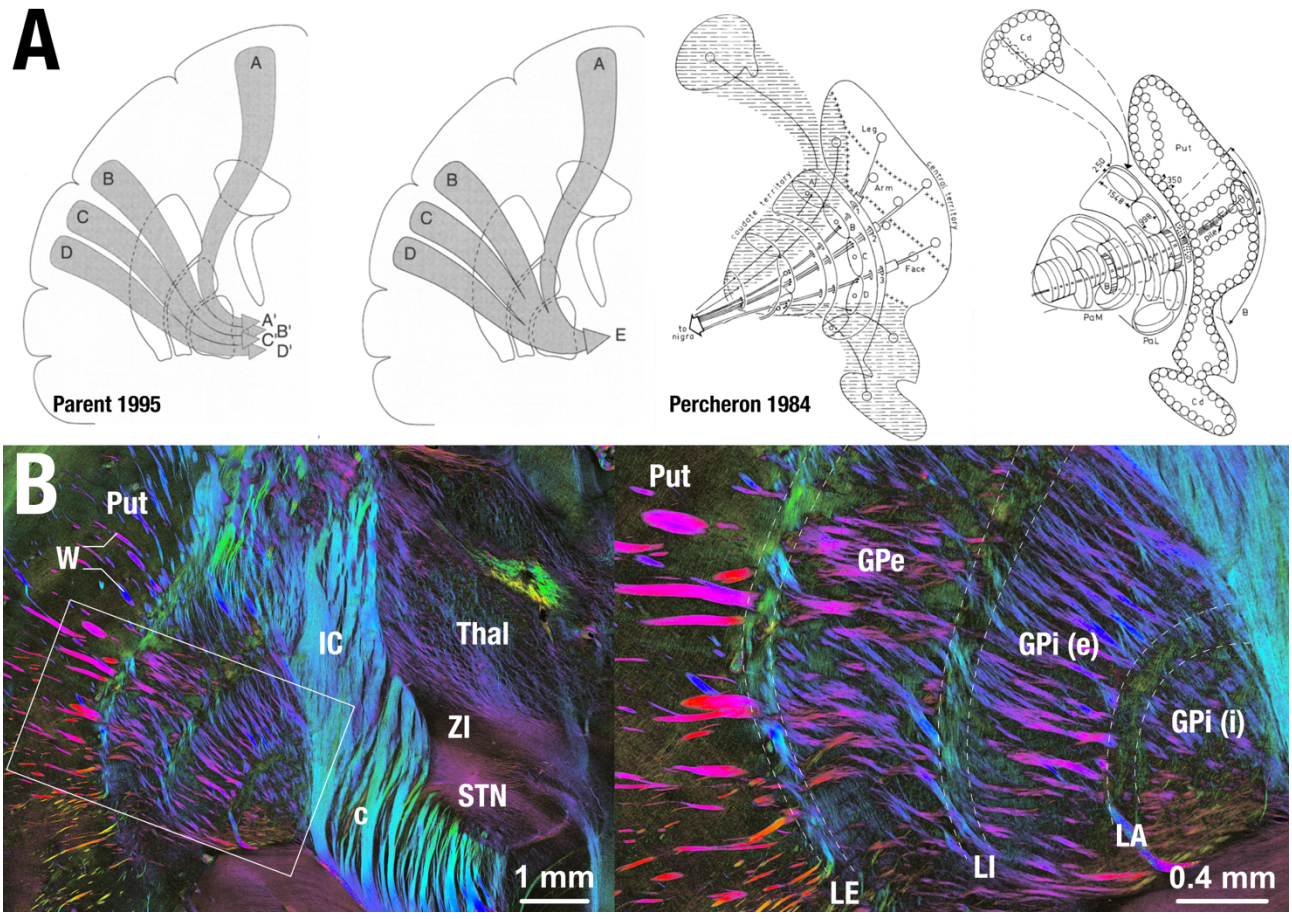

Figure S1: *Anatomical considerations. A) As two basic frameworks, the parallel loops and funnel concepts were reviewed by Parent et al. 1995. The concepts are not competing, rather, both are partly implemented by the corticostriatal and striatopallidofugal system of the basal ganglia. Information from different cortical sites (A-D) are partly kept segregated (leading to information sites in A'-D') but also integrated (leading to a joint information site E). Hence, the basal ganglia both integrate information from cortical sites but partly keep information separate. This was nicely illustrated by Percheron et al. 1984, showing receptive fields of pallidal neurons that are organized in disk-like fashion orthogonal to incoming striatal projections. Of note, size of each disk is constant, leading to higher degrees of integration in increasingly medial parts of the pallidum. Panels of original publications reproduced with permission. B) Polarized Light Imaging data acquired in the vervet*

monkey shows multiple stages of data compression and rewiring but also shows parallel organization of incoming loops. Image courtesy by Markus Axer and Karl Zilles, data from (16).

As mentioned, pallidothalamic projections – anatomically realized by the ansa and fasciculus lenticularis which merge within Forel's field H1 to form the fasciculus thalamicus (17) – traverse the GPi *parallel* to its maximal extent and predominantly project to the pallidal part of the ventroanterior nucleus of the thalamus (VAp; (Ilinsky *et al.*, 2018)). An older model claimed that the fasciculus lenticularis would integrate projections from the external part of the GPi while the ansa the ones from the internal part of the GPi. However, this model has been revised and it was suggested that the two tracts rather form a joint functional unit (17, 18). We will adopt this view here, i.e., subsummize ansa and fasciculus lenticularis as *pallidothalamic projections*.

DBS in our cohort was applied to a single node of this complex network: the GPi. With a GPi-centric view in mind, the network can be dramatically simplified to two fiber systems that traverse in *quasi-orthogonal direction* to each other – which is exactly what we aimed to leverage in the present study.

Table S1: Summary of regions involved in DBS network mapping results. Coordinates of peaks are given in MNI (mm) format with the R-value denoted in brackets. Abbreviations: ACC, anterior cingulate cortex; BA, Brodmann area; CBM, cerebellum; IFG, inferior frontal gyrus, ins., insula; IPL, inferior parietal lobule, MCC, midcingulate cortex; MFG, middle frontal gyrus; MTG, middle temporal gyrus; OL, occipital lobule; PCC, posterior cingulate cortex; PreCG, precentral gyrus; Prec, precuneus; PostCG, postcentral gyrus; SFG, superior frontal gyrus; SMA, supplementary motor area; SMG, supramarginal gurys; SNr, substantia nigra; STG, superior temporal gyrus; STN, subthalamic nucleus

Reg.	Hem.	Cervical R-map	Generalized R-map	Combined R-Map	Agreement Map
		Positive Peak Coordinates X/Y/Z (Value)			
ACC (BA 24, 32)	RH	16/38/22 (0.13)	2/36/12 (0.27)	16/38/20 (0.13)	16/38/20 (2.86)
	LH	-22/42/6 (0.19)	-4/36/10 (0.27)	-20/38/18 (0.18)	-20/38/20 (2.30)
CBM	RH	22/-92/-18 (0.39)	36/-94/-24 (0.33)	50/-78/-22 (0.25)	30/-32/-28 (5.35)
	LH	-22/-84/-18 (0.36)	-26/-36/-24 (0.30)	-36/-32/-30 (0.22)	-36/-32/-30 (4.56)
IFG (BA 46, 47)	RH	14/14/-26 (0.20)	16/16/-28 (0.34)	14/12/-26 (0.18)	14/14/-26 (4.31)
	LH	-16/16/-26 (0.21)	-22/22/-28 (0.20)	-16/16/-26 (0.13)	-16/16/-28 (2.37)
Ins. (BA 13)	RH	-	36/14/-10 (0.16)	42/-22/8 (0.06)	-
	LH	-46/-42/22 (0.09)	-28/18/-12 (0.19)	-34/26/0 (0.03)	-34/24/6 (0.08)
IPL (BA 39, 40)	RH	34/-62/48 (0.15)	46/-50/42 (0.10)	34/-62/48 (0.09)	40/-54/44 (0.69)
	LH	-34/-48/62 (0.22)	-64/-50/46 (0.13)	-38/-62/46 (0.09)	-46/-52/48 (0.70)
	RH	26/48/-22 (0.20)	28/38/-22 (0.22)	32/44/-22 (0.17)	28/38/-22 (2.53)

MFG (BA 9, 11)	LH	-20/46/-28 (0.27)	-30/36/-26 (0.21)	-30/44/-22 (0.15)	-20/44/-28 (2.40)
Midbrain	RH	14/-24/-22 (0.29)	10/-12/-10 (0.30)	4/-34/-12 (0.22)	12/-16/-10 (3.55)
	LH	-18/-14/-8 (0.23)	-8/-12/-14 (0.28)	-4/-34/-12 (0.21)	-4/-34/-12 (3.30)
OL (BA 17, 18)	RH	16/-104/2 (0.39)	22/-102/-8 (0.25)	20/-98/-12 (0.24)	20/-100/-12 (5.23)
	LH	-24/-98/-6 (0.39)	-12/-102/-12 (0.33)	-22/-100/-6 (0.22)	-22/-100/-8 (4.17)
PCC (BA 23, 30, 31)	RH	2/-70/18 (0.30)	2/-40/20 (0.19)	4/-66/8 (0.19)	2/-62/8 (3.05)
	LH	-20/-58/12 (0.32)	-4/-60/12 (0.24)	-4/-62/12 (0.19)	-4/-60/8 (3.27)
Prec. (BA 7, 19, 31)	RH	22/-80/48 (0.36)	10/-66/36 (0.14)	2/-72/54 (0.14)	14/-62/32 (1.98)
	LH	-32/-82/40 (0.34)	-40/-64/44 (0.25)	-6/-70/58 (0.13)	-18/-56/32 (2.46)
SFG (BA 11)	RH	24/48/-24 (0.21)	22/42/-24 (0.20)	24/46/-24 (0.13)	22/42/-24 (2.00)
	LH	-24/50/-24 (0.24)	-24/42/-24 (0.20)	-28/44/-24 (0.11)	-22/42/-28 (2.14)
SMA (BA 6)	RH	30/6/64 (0.12)	50/18/52 (0.15)	28/6/62 (0.06)	22/12/70 (0.32)
	LH	-32/-6/70 (0.21)	-46/18/58 (0.24)	-32/6/68 (0.09)	-38/12/64 (0.67)
SNr	RH	14/-20/-6 (0.14)	10/-24/-12 (0.28)	14/-20/-8 (0.18)	10/-18/-10 (2.92)
	LH	-16/-18/-6 (0.17)	-10/-12/-10 (0.26)	-18/-22/-6 (0.16)	-12/-22/-12 (2.32)
STN	RH	12/-16/-8 (0.16)	10/-14/-8 (0.23)	12/-16/-8 (0.17)	12/-16/-8 (2.84)
	LH	-14/-16/-8 (0.16)	-10/-12/-8 (0.19)	-14/-16/-8 (0.12)	-12/-16/-8 (1.27)
		Negative Peak Coordinates X/Y/Z (Value)			
IFG (BA 10, 47)	RH	18/24/-30 (-0.30)	42/56/-6 (-0.23)	58/36/-8 (-0.17)	46/50/-6 (-3.12)
	LH	-36/30/-10 (-0.35)	-44/60/-8 (-0.22)	-56/42/-16 (-0.19)	-56/42/-16 (-3.50)
MCC (BA 24)	RH	6/-2/34 (-0.32)	6/-4/34 (-0.19)	2/22/-12 (-0.13)	20/-14/44 (-1.92)
	LH	-6/2/34 (-0.34)	-6/0/34 (-0.22)	-6/22/-12 (-0.13)	-16/-12/42 (-1.97)
MTG (BA 19, 21, 37)	RH	46/0/-40 (-0.24)	46/-64/2 (-0.31)	62/-66/0 (-0.18)	66/-56/-2 (-3.05)
	LH	-48/0/-40 (-0.26)	-58/-60/-8 (-0.35)	-68/-54/-6 (-0.20)	-68/-54/-6 (-4.20)
PostCG (BA 3, 1, 2)	RH	50/-22/32 (-0.14)	54/-26/44 (-0.29)	22/-22/52 (-0.14)	54/-24/42 (-2.05)
	LH	-70/-10/24 (-0.13)	-52/-24/42 (-0.30)	-52/-24/40 (-0.12)	-70/-8/24 (-1.51)
PreCG (BA 3, 4)	RH	58/-12/30 (-0.13)	18/-22/58 (-0.22)	40/-16/50 (-0.16)	60/-14/36 (-1.56)
	LH	-70/-2/24 (-0.13)	-60/-14/42 (-0.20)	-24/-20/56 (-0.11)	-70/-6/26 (-1.50)
SFG. (BA 6 11)	RH	2/32/54 (-0.31)	18/48/-28 (-0.22)	4/32/54 (-0.17)	4/32/46 (-1.32)
	LH	-8/30/56 (-0.33)	-18/56/-26 (-0.20)	-8/30/56 (-0.19)	-8/32/56 (-1.91)
SMG (BA 40)	RH	52/-48/26 (-0.23)	60/-54/28 (-0.13)	64/-52/28 (-0.17)	62/-52/28 (-1.92)
	LH	-70/-46/24 (-0.20)	-62/-46/24 (-0.16)	-66/-46/24 (-0.18)	-64/-46/24 (-2.07)
STG (BA 13, 22)	RH	42/-44/22 (-0.26)	42/-58/16 (-0.21)	50/-30/-22 (-0.18)	46/4/-10 (-2.53)
	LH	-74/-42/8 (-0.28)	-56/14/-12 (-0.18)	-74/-42/8 (-0.20)	-74/-42/8 (-2.80)

Replication of fiber filtering results using an additional atlas

Results from fiber filtering are dependent on the pathway atlas used – for the simple reason that i) only tracts present in the atlas may be associated with clinical improvements and ii) in case tracts are presented in anatomically incongruent fashion, this would lead to similarly incongruent results. While the main atlas used in this publication was curated by four world experts in the field of subcortical anatomy and demonstrates unprecedented anatomical detail (19), aforementioned limitations could still apply to our results. Unfortunately, this atlas is unique in multiple ways, and we are not aware of a second, similar dataset of comparable detail. However, going into a similar direction to create an expert-delineated subcortical tract atlas, Middlebrooks and colleagues recently published the DBS Tractography Atlas (20) which is based on deterministic tractography built on data (21) from 1,000 healthy brains acquired within the human connectome project (22). Unfortunately, the atlas does not include comb fibers or axon-collaterals that accurately represent hyperdirect projections. It also represents the ansa and fasciculus lenticulares in a way that does not traverse within the pallidum, which prevents us from testing our main hypothesis (figure 1) based on this atlas. However, the more coarse-level results (figure 5A) could be reproduced (figure S2).

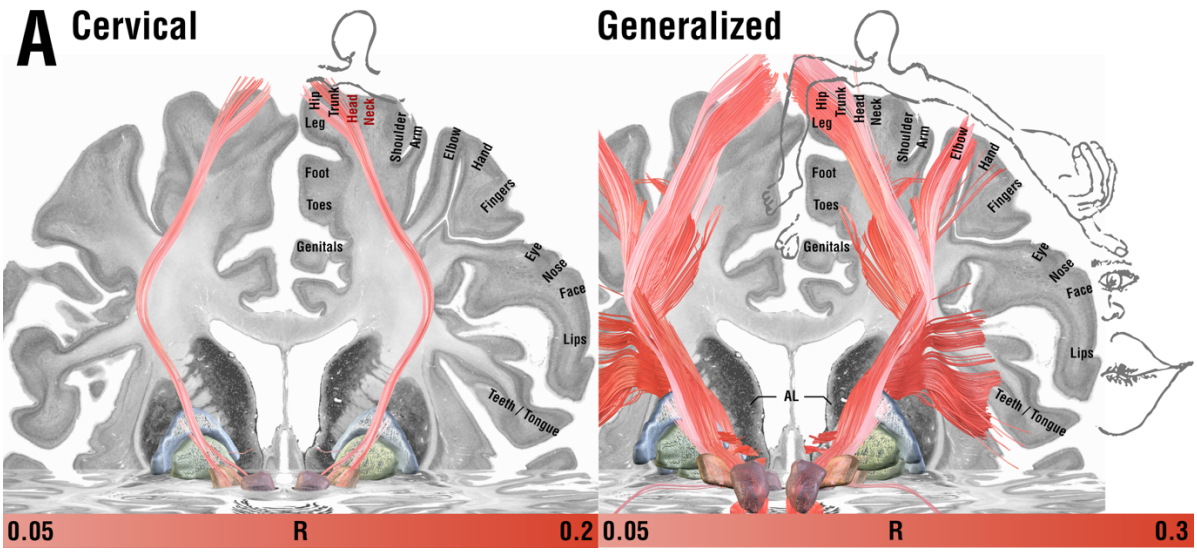

Figure S2: *Replication of somatotopy results using the DBS Tractography Atlas (20). As in the main analysis (based on the holographic Basal Ganglia Pathway Atlas (23)), cortical projections associated with optimal outcomes in cervical dystonia were limited to mesial origins which include the head and neck regions of the central homunculus. The ones associated with generalized dystonia instead showed a more widespread pattern and included the pallidothalamic projections (ansa/fasciculus lenticulares).*

References

1. G. E. Alexander, M. D. Crutcher, M. R. DeLong, Basal ganglia-thalamocortical circuits: parallel substrates for motor, oculomotor, "prefrontal" and "limbic" functions. *Prog. Brain Res.* **85**, 119–146 (1990).

2. H. Bergman, T. Wichmann, M. R. DeLong, Reversal of experimental parkinsonism by lesions of the subthalamic nucleus. *Science* **249**, 1436–1438 (1990).

3. J. Volkmann, C. Daniels, K. Witt, Neuropsychiatric effects of subthalamic neurostimulation in Parkinson disease. *Nat. Publ. Group* **6**, 487–498 (2010).

4. L. W. Swanson, Cerebral hemisphere regulation of motivated behavior. *Brain Res.* **886**, 113–164 (2000).

5. K. Gurney, T. J. Prescott, P. Redgrave, A computational model of action selection in the basal ganglia. I. A new functional anatomy. *Biol. Cybern.* **84**, 401–410 (2001).

6. M. Deffains, *et al.*, Subthalamic, not striatal, activity correlates with basal ganglia downstream activity in normal and parkinsonian monkeys. *eLife* **5**, 4854 (2016).

7. A. Nambu, H. Tokuno, M. Takada, Functional significance of the cortico–subthalamo–pallidal 'hyperdirect' pathway. *Neurosci. Res.* **43**, 111–117 (2002).

8. C. C. McIntyre, P. J. Hahn, Network perspectives on the mechanisms of deep brain stimulation. *Neurobiol. Dis.* **38**, 329–337 (2010).

9. G. Percheron, J. Yelnik, C. François, A Golgi analysis of the primate globus pallidus. III. Spatial organization of the striato-pallidal complex. *J. Comp. Neurol.* **227**, 214–227 (1984).

10. A. Parent, L. N. Hazrati, Functional anatomy of the basal ganglia. II. The place of subthalamic nucleus and external pallidum in basal ganglia circuitry. *Brain Res. Brain Res. Rev.* **20**, 128–154 (1995).

11. T. Kita, H. Kita, The Subthalamic Nucleus Is One of Multiple Innervation Sites for Long-Range Corticofugal Axons: A Single-Axon Tracing Study in the Rat. *J. Neurosci. Off. J. Soc. Neurosci.* **32**, 5990–5999 (2012).

12. D. Coudé, A. Parent, M. Parent, Single-axon tracing of the corticosubthalamic hyperdirect pathway in primates. *Brain Struct. Funct.* **223**, 3959–3973 (2018).

13. S. A. K. Wilson, An Experimental Research into the Anatomy and Physiology of the Corpus Striatum. *Brain J. Neurol.* **36**, 427–492 (1914).

14. A. Horn, *et al.*, Teaching NeuroImages: In vivo visualization of Edinger comb and Wilson pencils. *Neurology* **92**, e1663–e1664 (2019).

15. L. Edinger, *Vorlesungen über den Bau der nervösen Centralorgane des Menschen und der Thiere. Für Ärzte und Studirende.* (F.C.W. Vogel, 1896).

16. H. Takemura, *et al.*, Anatomy of nerve fiber bundles at micrometer-resolution in the vervet monkey visual system. *eLife* **9** (2020).

17. C. Neudorfer, M. Maarouf, Neuroanatomical background and functional considerations for stereotactic interventions in the H fields of Forel. *Brain Struct. Funct.* **223**, 17–30 (2018).

18. M. Parent, A. Parent, The pallidofugal motor fiber system in primates. *Park. Amp Relat. Disord.* **10**, 203–211 (2004).

19. A. M. Noecker, *et al.*, StimVisionv2: Examples and Applications in Subthalamic Deep Brain Stimulation for Parkinson's Disease. *Neuromodulation Technol. Neural Interface* **12**, 75–11 (2021).

20. E. H. Middlebrooks, *et al.*, Neuroimaging Advances in Deep Brain Stimulation: Review of Indications, Anatomy, and Brain Connectomics. *AJNR Am. J. Neuroradiol.*, 1–11 (2020).

21. F.-C. Yeh, *et al.*, Population-averaged atlas of the macroscale human structural connectome and its network topology. *NeuroImage* **178**, 57–68 (2018).

22. D. C. Van Essen, *et al.*, The Human Connectome Project: A data acquisition perspective. **62**, 2222–2231 (2012).

23. M. V. Petersen, *et al.*, Holographic Reconstruction of Axonal Pathways in the Human Brain. *Neuron*, 1–13 (2019).